Korean J. Chem. Eng., 33(11), 3267-3272 (2016)
DOI: 10.1007/s11814-016-0181-8

pISSN: 0256-1115
eISSN: 1975-7220

Thermal decomposition kinetics and characterization of poly(butylene 2,5-furandicarboxylate)/Cloisite 30B composites

Bong-Sang Cho*,, Myeong-Jun Kim***, Suel-Ki Jung***, and Shin Choon Kang*,†**

*Department of Chemical Engineering, College of Engineering Science, Hanyang University, Ansan-si, Gyeonggi-do 15588, Korea
**Human and Culture Convergence Technology R&BD Group, Korea Institute of Industrial Technology, Ansna-si, Gyeonggi-do 15588, Korea
***Thermal & Fluid System R&D Group, Korea Institute of Industrial Technology, Cheonan-si, Chungcheongnam-do 31056, Korea
(*Received 21 June 2015 • accepted 28 June 2016*)

Abstract−2,5-Furandicarboxylic acid (FDCA) was synthesized by $KMnO_4$ oxidation of 2,5-dihydroxymethylfuran (DHMF) derived from biomass. The poly(butylene 2,5-furandicarboxylate)/Cloisite 30B (PBF30B) composites were prepared by esterification and polycondensation of FDCA with 1,4-butane diol. PBF30B composites containing 1, 2, and 4 phrs Cloisite 30B were prepared. The FDCA and PBF30B composites were characterized by Fourier transform infrared spectroscopy (FT-IR), and X-ray diffractometry (XRD). The thermal decomposition kinetics of PBF 30B composites were studied by thermogravimetric analysis (TGA) under conditions of 1, 2, 4, 6, and 8 °C/min. The activation energies of PBF30B composites were investigated by Arrhenius regression, the Flynn-Wall-Ozawa method, original Vyazovkin method and advanced iso-conversion method. From the standpoint of activation energy for the decomposition of PBF 30B composites, the different kinetic methods shared the same tendency. The Vyazovkin method yielded the maximum activation energies of PBF30B composites containing 1, 2, and 4 phrs Cloisite 30B which were 190, 140, and 160 kJ/mol, respectively.

Keywords: Poly(butylene 2,5-furandicarboxylate), Cloisite 30B, TGA, Thermal Decomposition Kinetics

INTRODUCTION

Approximately 95% of all manufactured chemicals currently originate from fossil resources. However, due to dwindling of these resources, surging energy demand and global warming, there has been an increasing focus on the development of technologies that facilitate the conversion of bio-renewable energy source into transportation fuels [1]. 5-Hydroxymethyl-2-furaldehyde (HMF) and 2-furaldehyde convert to form by-products under similar conditions for use in polymer materials [2-5]. We demonstrate that the esterification of platform molecules such as 2,5-furandicarboxylic acid (FDCA) can be effective for the conversion of platform molecules into renewable base chemicals by the simplest reagents, which can be used as polymer building blocks. FDCA has been proposed as a replacement for terephthalic acid used as a monomer in polyethylene terephthalate (PET) plastics that are widely used in beverage packaging [6,7].

Polymer nanocomposites have attracted great attention worldwide due to properties such as modulus, strength, toughness and barrier, which are far superior to those of conventional microcomposites and comparable to those of metal. A broad spectrum of polymer properties can be improved by nanocomposite technology such as mechanical, thermal barrier, durability, chemical stability, flame retardancy, scratch/wear resistance, biodegradability as well as optical, magnetic and electrical properties [8-11]. The thermal degradation of polymer nanocomposites is an important phenomenon. Kinetic analyses provide information on energy barriers of the degradation process and are used to explain the mechanism of degradation. Degradation kinetic parameters can be obtained from dynamic experiments by means of different methods [12-15].

We synthesized FDCA and poly(butylene 2,5-furandicarboxylate)/Cloisite 30B (PBF30B) composites. The PBF30B composites were synthesized by esterification and polycondensation of FDCA with 1,4-butanediol. PBF30B composites containing 1, 2, and 4 phr Cloisite 30B were prepared. The FDCA and PBF 30B composites were characterized by the Fourier transform infrared spectroscopy (FT-IR), and X-ray diffractometry (XRD). The thermal decomposition kinetics of PBF30B composites were studied by thermogravimetric analysis (TGA) under conditions of 1, 2, 4, 6, and 8 °C/min. The Arrhenius integration, the Flynn-Wall-Ozawa method, the advanced isoconversion method, and the Vyazovkin methods were used to evaluate the kinetic parameters of PBF30B composites.

EXPERIMENTAL

1. Materials

2,5-Dihydroxymethylfurfural [DHMF; Pennakem; 97%], 1,4-

†To whom correspondence should be addressed.
E-mail: kangsc@hanyang.ac.kr

buthanediol [BDO; Aldrich; 99%], titanium(IV) (triethanolaminato) isopropoxide [Tyzor; Aldrich], sodium hydroxide [Samchun Chemical Co.; 99%], hydrochloric acid [Samchun Chemical Co.; 35-37%], and potassium permanganate [Samchun Chemical Co.; 99%] were used as received.

2. Synthesis

2-1. Synthesis of 2,5-Furandicarboxylic Acid (FDCA)

DHMF (5.12 g, 0.04 mol) was reacted with potassium permanganate (22.12 g, 0.14 mol) as a oxidation reagent in a 10% aqueous solution of sodium hydroxide at 25 °C for 10 min. After the manganese oxide was filtered through a celite filter, the filtrate was stirred by adding hydrochloric acid until the pH fell to below 1 and the temperature to room temperature. While hydrochloric acid was added, the temperature of the solution rose, gas bubbles formed, and the products precipitated to the bottom of the flask. The precipitate was filtered and washed with distilled water, then dried in vacuum oven to give pure FDCA.

2-2. Preparation of Poly(butylene 2,5-furandicarboxylate)/Cloisite 30B (PBF30B) [16]

Under melt polymerization conditions, FDCA (5 g, 0.032 mol), Cloisite 30B (1, 2, and 4 phr), and 2.3 equivalents of BDO in the presence of 200 ppm Tyzor were stirred under nitrogen at 80 °C for 30min and reacted in a transesterification step at 180 °C for 2 hrs, after which polycondensation was carried out at 230 °C for 48 hours. To obtain polymers of high molecular weight, the polymers were dissolved in phenol : 1,1,2,2-tetrachloroethane (5 : 5) mixture, and then the mixtures were reprecipitated in methanol. The product was filtered, and dried under reduced pressure at 100 °C.

3. Measurements

Fourier transform infrared spectroscopy (FT-IR) was performed by using an Avator 360 ESP (Nicolet Instrument Corp). The FT-IR was encased in dry nitrogen, which reduced the risk of atmospheric water or carbon dioxide contamination of the spectra or samples. All spectra were recorded at 25 °C with a resolution of 4 cm^{-1} in the spectral range of 4,000-400 cm^{-1} for a total of 128 scans and corrected against the background spectrum of air.

XRD was performed at room temperature using a Rigaku model D/MAX-2500H diffractometer. The X-ray beam was a K-absorption filter Cu$K\alpha$ (λ=0.154 nm) with radiation operated at 40 kW and 30 mA. Data were obtained from 3° to 13° (2θ) at a rate of 1°/min.

The results of thermogravimetric analysis (TGA) were recorded using a TA Instrument TGA-2050 in the temperature range from 25 to 800 °C at heating rates of 1, 2, 4, 6, and 8 °C/min under a nitrogen atmosphere with a sample weight of about 10 mg.

4. Kinetic Analysis

4-1. The Arrhenius Regression (Differential Method) [17]

For nonisothermal thermogravimetric analysis, the conversion fraction at any temperature is

$$\alpha = \frac{m_0 - m_T}{m_0 - m_\infty} \tag{1}$$

where, m_0 is the initial sample weight, m_T is the sample weight at temperature, T, and m_∞ is the final sample weight. The decomposition kinetics of PBF30B composites containing 1, 2, and 4 phr Cloisite 30B can be expressed as follows:

$$\frac{d\alpha}{dt} = kf(\alpha) \tag{2}$$

$$g(\alpha) = kt \tag{3}$$

where $f(\alpha)$ is the differential reaction model and $g(\alpha)$ is the integral reaction model. The temperature dependence of the rate constant, k is represented by the Arrhenius equation:

$$k = Ae^{-E_a/RT} \tag{4}$$

where A is the pre-exponential factor, E_a is activation energy, R is the gas constant, and T is absolute temperature. Substitution of Eq. (4) into Eqs. (2) and (3) results in the following equations for the differential model and integral model respectively:

$$\frac{d\alpha}{dt} = Ae^{-E_a/RT} f(\alpha) \tag{5}$$

$$g(\alpha) = Ae^{-E_a/RT} \cdot t \tag{6}$$

Using the Eq. (5), the activation energy is then calculated from the slope of a plot of the natural logarithm of $d\alpha/dt$ versus 1/T.

4-2. The Vyazovkin and Advanced Isoconversional Method [18]

The kinetic parameters of the integral isoconversional method were based on the assumption that the reaction model in Eq. (3) was not dependent on temperature. According to the Vyazovkin (VYZ) method, for a set of n experiments performed at various heating rates (β), the activation energy (E_a) at any specific value of decomposition (α) can be determined by minimizing the function $\Phi(E_a)$:

$$\Phi(E_a) = \Sigma_{i=1}^{n} \Sigma_{j \neq i}^{n} \frac{J[E_{a\alpha}, T_i(t_\alpha)]}{J[E_{a\alpha}, T_j(t_\alpha)]} \tag{7}$$

In Eq. (7), the temperature integral is represented as:

$$J[E_{a\alpha}, T_i(t_\alpha)] = \int_0^{t_\alpha} \exp\left(-\frac{E_{a\alpha}}{RT(t)}\right) dt \tag{8}$$

Vyazovkin developed an advanced isoconversional (AIC) method [19] that involves integration over smaller time intervals. Therefore, Eq. (8) can be altered to yield the following equation:

$$J[E_{a\alpha}, T_i(t_\alpha)] = \int_{t_\alpha - \Delta\alpha}^{t_\alpha} \exp\left(-\frac{E_{a\alpha}}{RT(t)}\right) dt \tag{9}$$

The integration is carried out the entire time interval 0~t_α in VYZ M but the individual interval $t_{\alpha-\Delta\alpha}$~t_α in AIC M.

4-3. Flynn-Wall-Ozawa (FWO) Method [20]

In a nonisothermal system, $f(\alpha)$ can be expressed in integral form as the function $g(\alpha)$ as follows:

$$g(\alpha) = \int_0^{\alpha} \frac{d\alpha}{f(\alpha)} = \frac{A}{\beta} \cdot \int_0^{T} e^{-\frac{E_a}{RT}} dT = \frac{AE_a}{\beta R} p(x) \tag{10}$$

The p(x) function was described by Flynn, Wall, and Ozawa using Doyle's approximation as follows [21]:

$$p(x) \cong 0.0048 e^{-1.0516x} \tag{11}$$

$$\ln \beta_i = \ln\left(\frac{A_\alpha E_\alpha}{Rg(\alpha)}\right) - 5.331 - 1.0516 \frac{E_\alpha}{RT_\alpha} \tag{12}$$

where subscripts i and α denote a given heating rate and value of

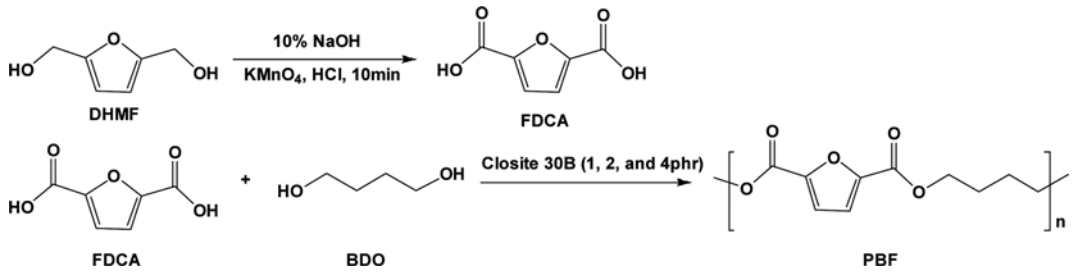

Scheme 1. The overall reaction of FDCA and PBF.

conversion, respectively. $g(\alpha)$ is the integral function of conversion. The activation energy is then calculated from the slope of a plot of the natural logarithm of the heating rate $\ln\beta_i$ versus $1/T_\alpha$.

The activation energies of PBF 30B composites were calculated by using the Arrhenius regression, the VYZ method, AIC method, and FWO method with the MATLAB program.

RESULTS AND DISCUSSIONS

The overall reaction schemes to synthesize FDCA and PBF 30B are shown in Scheme 1. The endpoint of the FDCA reaction was characterized by FT-IR and confirmed by the disappearance of the methylene group (-CH_2-) peak for DHMF and the appearance of a carbonyl group (-C=O) for FDCA. The IR spectra of DHMF and FDCA are shown in Fig. 1(a)-(b). In Fig. 1(a), the stretching vibration for the -CH_2- bond of DHMF appears at approximately 2,900 cm^{-1} and the stretching vibrations for the -C=C group and =C-H of furan ring are at 1,650 cm^{-1} and 3,050 cm^{-1}, respectively. However, the peak at 2,900 cm^{-1} disappears and the stretching vibration for the carbonyl group (-C=O-) bond of FDCA appears at approximately 1,715 cm^{-1} as shown in Fig. 1(b). The some extra absorption peaks appear for DHMF and FDCA, furan breathing around 1,023 cm^{-1} and furan ring bending at 956 cm^{-1}, and 750 cm^{-1}.

The diffusion of Cloisite30B was confirmed by XRD. Clay and organoclays show characteristic peaks in XRD analysis due to their regular layered structures, which is indicative of platelet separation or d-spacing. Using the peak width at half maximum height and peak position (2θ) in the XRD spectra the interlayer space can be calculated by Bragg's law.

$$\sin\theta = n\lambda/2d$$

where λ is the wave length of X-ray radiation used in the diffraction experiments, d is the space between layers in the clay lattice and θ is the measured diffraction angle.

Fig. 2 shows the XRD spectra of Cloisite 30B, FDCA, and PBF 30B composites. XRD was used to characterize the PBF 30B composites. Cloisite 30B is the organically modified sodium in MMT with a quaternary ammonium salt. The PBF spectrum presents sharp peaks at 2-theta peak of 17.7, and 24.5 degree [22]. The Cloisite 30B has a characteristic 2-theta peak of 4.9 degrees corresponding to the interlayer space of 1.8 nm, and the FDCA has a characteristic 2-theta peak of 10.6 degrees. PBF30B composites containing 2 and 4 phr have a characteristic 2-theta peak of 6.5 degrees, which indicates a collapse in the clay layered structure. TGA was carried out on the PBF30B composites to investigate their thermal stability, decomposition temperature, and decomposition mechanism. Fig. 3 shows the weight loss-temperature (TG) curves and the derivatives of conversion-temperature (DTG) curves obtained from TGA curves of the PBF30B composites containing Cloisite 30B (a) 1 phr (b) 2 phr and (c) 4 phr.

In the DTG curves, the curves shifted to higher temperature as the heating rate was increased due to the shorter time required to reach a given temperature at a faster heating rate [23]. The TG curves of PBF30B composites displayed distinct regions of weight loss in all samples. The first decomposition occurred between 320 and 380 °C. The first-stage decomposition occurred due to cleavage of

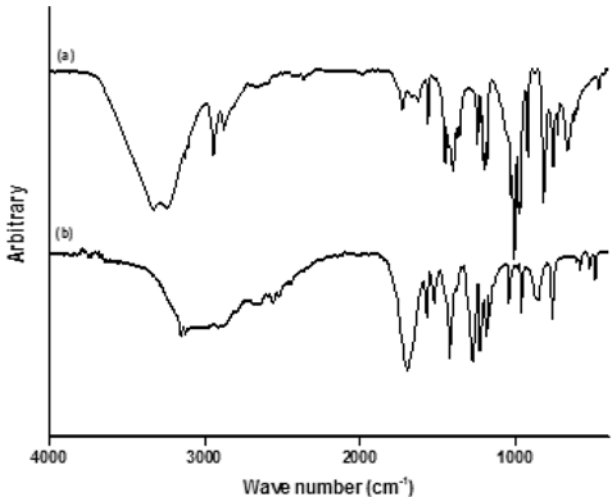

Fig. 1. FT-IR spectra of (a) DHMF and (b) FDCA.

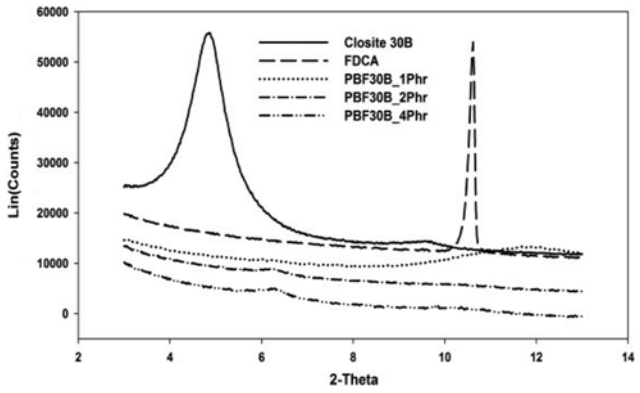

Fig. 2. XRD spectra of Cloisite30B, FDCA, and PBF30B composites.

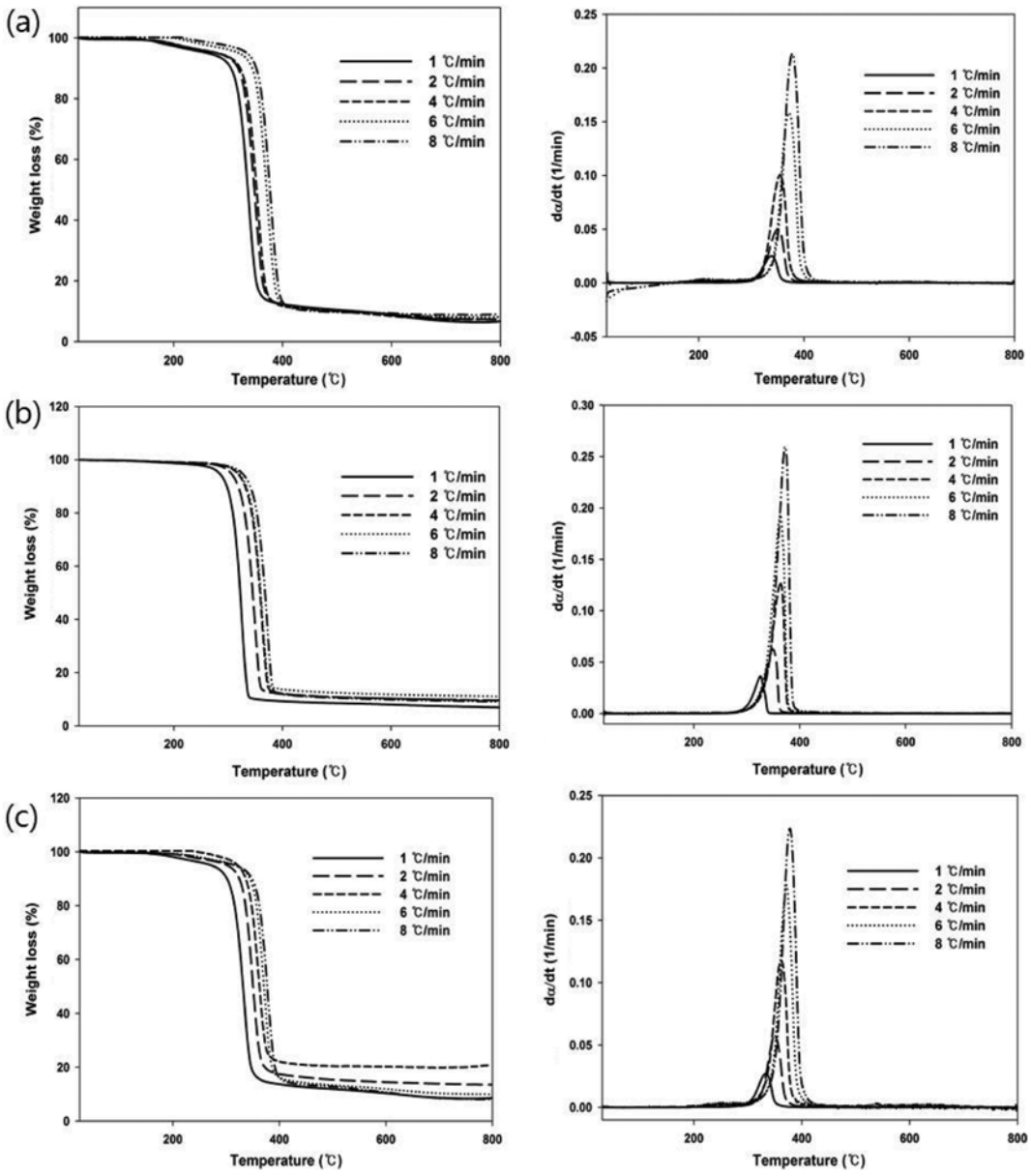

Fig. 3. The weight loss-temperature curves and derivatives of conversion-temperature plots obtained from TGA curves of PBF30B composites: (a) 1 phr, (b) 2 phr, and (c) 4 phr.

the PBF. The purpose of these thermal decomposition experiments was to obtain kinetic parameters including activation energy to enable prediction of the thermal decomposition process. The degree of conversion rate as a function of heating rate was obtained from the experimental data. The nonisothermal method was used to analyze TG/DTG curves and to obtain the value for the kinetic parameters. From the result of TGA, the activation energies were determined by various methods. The different calculation methods (Arrhenius regression, VYZ, AIC, and FWO method) were applied in this study.

The activation energies can be calculated from the slope of the FWO plot at different conversions for PBF30B composites as shown in Fig. 4. The regression curve was generated by the least square method. The calculated activation energies of PBF30B composites decomposition obtained by the FWO method are summarized in Table 1.

Based on data shown in Fig. 4 and Table 1, the activation energies of PBF30B composites containing 1, 2, and 4 phr Cloisite 30B obtained using the FWO method are 153.9, 139.1 and 143.1 kJ/mol, respectively.

Fig. 5 shows the dependence of the activation energy on the conversion for the decomposition of PBF30B composites. The Arrhenius regression (Dif. method) and AIC method showed some fluctuation of activation energy as a function of the extent of reaction; it is due to the isoconversion line t_α (Dif. method) and with integration over small time segments $t_{\alpha-\Delta\alpha}$ to t_α (AIC method). On the other hand, the activation energy calculation of the FWO method used the approximation function, and that of the VYZ

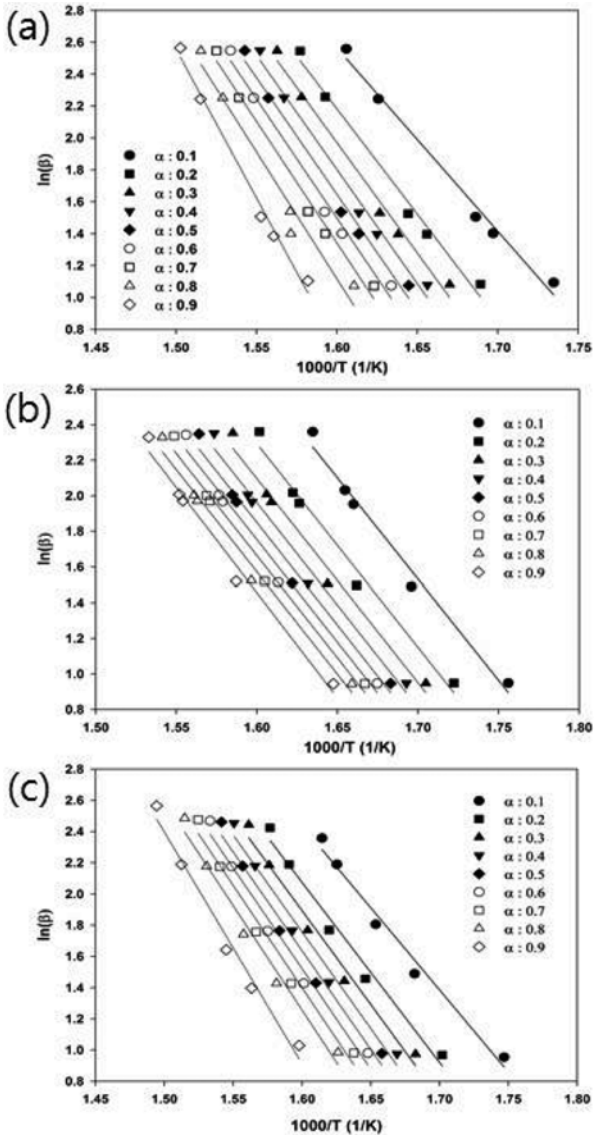

Fig. 4. The plot of ln(β) vs. T^{-1} for calculating the activation energies by FWO method of producing PBF30B composites: (a) 1 phr, (b) 2 phr, and (c) 4 phr.

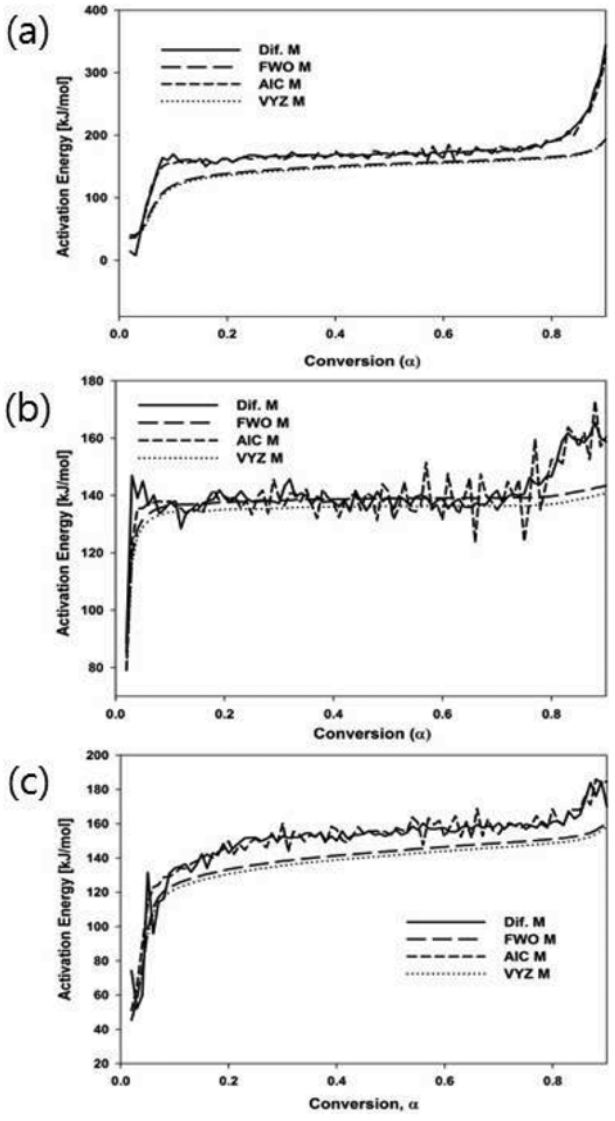

Fig. 5. Dependence of activation energy on the extent of conversion for PBF30B composites: (a) 1 phr (b) 2 phr and (c) 4 phr.

Table 1. The activation energies of PBF30B composites decomposition obtained by the FWO method

Degree of conversion (α)	Activation energy (kJ/mol)		
	(a) 1 phr	(b) 2 phr	(a) 4 phr
0.1	119.9	136.7	124.3
0.2	138.5	137.7	133.4
0.3	145.5	138.2	138.3
0.4	150.5	138.7	141.5
0.5	154.1	139.0	144.0
0.6	157.3	139.0	146.4
0.7	160.8	139.1	148.6
0.8	165.2	139.7	151.1
0.9	193.5	143.4	160.5
Average	153.9	139.1	143.1

method used the accumulated time interval 0~t_α; then the activation energy variations were smooth. The activation energy deviations were smaller since integrated data points were used to estimate the activation energies for each given α. Accordingly, we proceeded with data analysis by the VYZ method. In Fig. 5(a), the VYZ method curve shows the one decomposition stage for the varying activation energies. The activation energy sharply increased to 118 kJ/mol for the conversion of $0<\alpha<0.1$ due to the influence of humidity or residual monomer. The activation energy slightly increased from 118 kJ/mol to 168 kJ/mol for $0.1<\alpha<0.8$ (first decomposition stage) and slightly increased from 168 kJ/mol to 182 kJ/mol for $\alpha>0.8$. In Fig. 5(b), the activation energy sharply increased to 134 kJ/mol for conversion of $0<\alpha<0.1$ due to the influence of humidity or residual monomer. The activation energy slightly increased from 134 to 136 kJ/mol for $0.1<\alpha<0.8$. At $\alpha>0.8$, the activation energy increased from 136 to 140 kJ/mol. In Fig. 5(c), the activation energy sharply increased to 121 kJ/mol for the

conversion of $0<\alpha<0.1$ due to the influence of humidity or residual monomer. The activation energy slightly increased from 121 to 148 kJ/mol for $0.1<\alpha<0.8$. At $\alpha>0.8$, the activation energy increased from 148 to 158 kJ/mol. The effect of increasing the activation energy during decomposition was amplified because the volatilization of larger chain fragments implies higher volatilization energies. The activation energies of PBF30B composites, which were determined by different kinetic methods, were similar im tendency. The maximum activation energies of PBF30B composites containing 1, 2, and 4 phr Cloisite30B were 190, 140, and 160 kJ/mol, respectively.

CONCLUSIONS

We synthesized FDCA by $KMnO_4$ oxidation of DHMF and prepared PBF30B composites by esterification and polycondensation of FDCA with 1,4-butane diol containing 1, 2, and 4 phrs Cloisite 30B. The FDCA and PBF30B were characterized by FT-IR, and XRD. The thermal decomposition kinetics of PBF30B composites were investigated by Arrhenius regression, the Flynn-Wall-Ozawa method, the original Vyazovkin method and advanced iso-conversional method. The activation energy and decomposition behavior were calculated from TGA and DTG results by several kinetic models. The kinetic analysis was performed with model free methods such as Vyazovkin method, advanced iso-conversional method, and Flynn-Wall-Ozawa method. Throughout all of the methods, a similar tendency was observed regarding change of activation energy in each conversion. From the result of activation energy on the conversion for the decomposition of PBF30B containing 1, 2, and 4 phrs Cloisite 30B, in spite of different calculation methods, the activation energy variations are similar. The maximum activation energies of PBF30B containing 1, 2, and 4 phrs Cloisite 30B in the Vyazovkin method were 190, 140, and 160 kJ/mol, respectively.

REFERENCES

1. M. Dashtban, H. Schraft and W. Qin, *Int. J. Biol. Sci.*, **5**, 578 (2009).
2. P. E. Shaw, J. H. Tatum and R. E. Berry, *Carbohydr. Res.*, **5**, 266 (1967).
3. L. Cottier and G. Descotes, *Trends Heterocyc. Chem.*, **2**, 233 (1991).
4. H. Zhao, J. H. Holladay, H. Brown and Z. C. Zhang, *Science*, **316**, 1597 (2007).
5. Y. Román-Leshkov, C. J. Barrett, Z. Y. Liu and J. A. Dumesic, *Nature*, **447**, 982 (2007).
6. P. Verdeguer, N. Merat and A. Gaset, *J. Mol. Catal.*, **85**, 327 (1993).
7. J. N. Chheda, Y. Román-Leshkov and J. A. Dumesic, *Green Chem.*, **9**, 342 (2007).
8. I. Armentano, M. Dottori, E. Fortunati, S. Mattioli and J. M. Kenny, *Polym. Degrad. Stab.*, **95**, 2126 (2010).
9. P. Cosoli, G. Scocchi, S. Pricl and M. Fermaglia, *Micropor. Mesopor. Mater.*, **107**, 169 (2008).
10. H. Ma, Z. Xu, L. Tong, A. Gu and Z. Fang, *Polym. Degrad. Stab.*, **91**, 2951 (2006).
11. J. K. Pandey, K. R. Reddy, A. P. Kumar and R. P. Singh, *Polym. Degrad. Stab.*, **88**, 234 (2005).
12. G. X. Chen and J. S. Yoon, *Polym. Degrad. Stab.*, **88**, 206 (2005).
13. R. Zong, Y. Hu, S. Wang and L. Song, *Polym. Degrad. Stab.*, **83**, 423 (2004).
14. Y. Zhang, Z. Xia, H. Huang and H. Chen, *Polym. Test.*, **28**, 264 (2009).
15. M. H. Yang, D. K. Tsay and J. H. Wang, *Polym. Test.*, **21**, 737 (2002).
16. J. A. Moore and J. E. Kelly, *Macromolecules*, **11**, 568 (1977).
17. J. H. Sharp and S. A. Wentworth, *Anal. Chem.*, **41**, 2060 (1969).
18. S. Vyazovkin, *J. Comput. Chem.*, **18**, 393 (1997).
19. S. Vyazovkin, *J. Comput. Chem.*, **22**, 178 (2001).
20. J. Opfermann and E. Kaisersberger, *Thermochim. Acta*, **203**, 167 (1992).
21. C. Doyle, *J. Appl. Polym. Sci.*, **5**, 285 (1961).
22. J. Zhu, J. Cai, W. Xie, P. H. Chen, M. Gazzano, M. Scandola and R. A. Gross, *Macromolecules*, **46**, 796 (2013).
23. T. Bril, P. Gongwer and G. Williams, *J. Phys. Chem.*, **98**, 12242 (1994).